



# Nanogram-scale boron isotope analysis through micro-distillation and Nu Plasma 3 MC-ICP-MS

César Nicolás Rodríguez-Díaz<sup>a,b,\*</sup>, Eduardo Paredes<sup>b</sup>, Leopoldo David Pena<sup>b</sup>, Isabel Cacho<sup>b</sup>, Carles Pelejero<sup>a,c</sup>, Eva Calvo<sup>a,\*\*</sup>

<sup>a</sup> Institut de Ciències del Mar, Consejo Superior de Investigaciones Científicas (CSIC), Passeig Marítim de la Barceloneta, 37-49, 08003 Barcelona, Spain

<sup>b</sup> GRC Geociències Marines, Dept. de Dinàmica de la Terra i de l'Oceà, Facultat de Ciències de la Terra, Universitat de Barcelona, C/Martí i Franquès s/n, 08028 Barcelona, Spain

<sup>c</sup> Institució Catalana de Recerca i Estudis Avançats (ICREA), Passeig Lluís Companys, 23, 08010, Barcelona, Spain

## ARTICLE INFO

### Keywords:

Boron isotopes  
MC-ICP-MS  
Micro-distillation  
Marine biogenic carbonates  
Paleo-pH

## ABSTRACT

The determination of boron isotopes ( $\delta^{11}\text{B}$ ) represents a powerful tool for a variety of applications such as the reconstruction of past ocean pH and atmospheric  $p\text{CO}_2$  from the analysis of marine biogenic carbonates. In recent years, MC-ICP-MS has gained popularity over other techniques thanks to its superior sample throughput and high ionization efficiency. This study evaluates, for the first time, the performance of the Nu Instruments Plasma 3 MC-ICP-MS for measuring  $\delta^{11}\text{B}$  using different sample introduction systems and detector configurations. The main goal is to provide a detailed methodology for nanogram-scale boron isotope analysis through a straightforward approach that can be easily adopted. Boron (B) purification from the carbonate matrix was performed through micro-distillation, using a temperature of 95 °C and a minimum heating duration of 15 h, allowing the full recovery of B from up to 3 mg of carbonate mass. We attained blank values (on average  $14 \pm 6$  pg, 1 SD,  $n = 27$ ) comparable to the lowest micro-distillation blanks reported in the literature. Three sample introduction systems were tested, and the  $30 \mu\text{L min}^{-1}$  nebuliser system outperformed the 50 and  $170 \mu\text{L min}^{-1}$  systems in terms of signal intensity per mass of B. Two detector configurations were used based on the total boron signal intensity achieved: (1) FC11/FC12, with two Faraday cups fitted to  $10^{11} \Omega$  and  $10^{12} \Omega$  amplifier resistors to detect  $^{11}\text{B}$  and  $^{10}\text{B}$  ion beams, respectively, and (2) FC12/IC, with which we investigated, for the first time, the feasibility of combining an ion counter for detecting  $^{10}\text{B}$ , and a Faraday cup fitted to a  $10^{12} \Omega$  amplifier for  $^{11}\text{B}$ . The FC12/IC configuration provided accurate results compared to the use of two Faraday cups for total boron signals lower than 0.35 V ( $\sim 12$  ng of B in the analysed solution). The proposed analytical procedure was validated through the analysis of several reference materials with varying boron amounts, including clam JCT-1, coral JCP-1, NIST RM 8301 Foram and Coral solutions, and boric acid ERM-AE121. Furthermore, the long-term reproducibility was assessed with two in-house standards (coral CLD-1 and foraminifera GINF-1), providing values of  $25.68 \pm 0.23$  ‰ (2SD,  $n = 53$ ; with 14–36 ng of B) and  $14.90 \pm 0.16$  ‰ (2SD,  $n = 12$ ; with 11–16 ng of B), respectively.

## 1. Introduction

Boron (B) is a light element that has two naturally occurring isotopes,  $^{10}\text{B}$  and  $^{11}\text{B}$ , with relative abundances of 19.9% and 80.1%, respectively [1]. There is a  $\sim 10$  % mass difference between these isotopes which leads to large isotopic fractionations during chemical and physical

processes. As a result, boron isotope ratio variations ( $\delta^{11}\text{B}$ ) ranging from  $-70$  ‰ [2] to  $+75$  ‰ [3], with respect to the commonly used NIST SRM 951a standard, have been measured in nature.

The analysis of  $\delta^{11}\text{B}$  proved to be a powerful tool for various geochemical applications such as tracing anthropogenic pollution sources [4], studying subduction zone processes [5], investigating

\* Corresponding author. Institut de Ciències del Mar, Consejo Superior de Investigaciones Científicas (CSIC), Passeig Marítim de la Barceloneta, 37-49, 08003 Barcelona, Spain.

\*\* Corresponding author.

E-mail addresses: [cnrodriguez@icm.csic.es](mailto:cnrodriguez@icm.csic.es) (C.N. Rodríguez-Díaz), [eduardo.paredes@ub.edu](mailto:eduardo.paredes@ub.edu) (E. Paredes), [lpna@ub.edu](mailto:lpna@ub.edu) (L.D. Pena), [icacho@ub.edu](mailto:icacho@ub.edu) (I. Cacho), [carles.pelejero@icrea.cat](mailto:carles.pelejero@icrea.cat) (C. Pelejero), [ecalvo@icm.csic.es](mailto:ecalvo@icm.csic.es) (E. Calvo).

<https://doi.org/10.1016/j.talanta.2023.125473>

Received 1 August 2023; Received in revised form 16 November 2023; Accepted 22 November 2023

Available online 28 November 2023

0039-9140/© 2023 The Authors. Published by Elsevier B.V. This is an open access article under the CC BY license (<http://creativecommons.org/licenses/by/4.0/>).

magmatism and hydrothermalism [6,7], and examining continental weathering [4]. Additionally,  $\delta^{11}\text{B}$  in biogenic carbonates, such as foraminifera and corals, is used as a proxy for reconstructing past oceanic pH and atmospheric  $p\text{CO}_2$ . In seawater, boron exists as two species in equilibrium, the proportion of them being pH dependent: trigonal boric acid  $\text{B}(\text{OH})_3$  and tetrahedral borate ion  $\text{B}(\text{OH})_4^-$ , the former being enriched in  $^{11}\text{B}$  compared to  $\text{B}(\text{OH})_4^-$ . Any change in seawater pH shifts this equilibrium and, consequently, leads to a modification of the isotopic signatures of these two forms, which is transferred to marine carbonates (being borate the dominant incorporated species). Hence, paleo-pH reconstructions can be generated from  $\delta^{11}\text{B}$  measurements in fossil carbonates, and past changes in atmospheric  $p\text{CO}_2$  can also be assessed in combination with alkalinity estimations (e.g., Refs. [8–10]). However, such seawater pH reconstructions require highly accurate  $\delta^{11}\text{B}$  determinations, with uncertainties typically better than 0.5 ‰, in order to resolve pH changes of around 0.1 units [10,11]. This accuracy can be obtained with Thermal Ionization Mass Spectrometry (TIMS), both in positive (PTIMS) and negative (NTIMS) modes, or with Multi-Collector Inductively Coupled Plasma Mass Spectrometry (MC-ICP-MS). From these techniques, PTIMS has been used for the analysis of corals [12,13], but it is not practical to analyse foraminifera samples, because large boron amounts (>100 ng) are required, whereas foraminifera samples typically contain a few tens of nanograms, at maximum. On the contrary, NTIMS [11] and MC-ICP-MS [14,15] can provide high precision  $\delta^{11}\text{B}$  values with only a few nanograms of boron, and the latter technique has gained popularity over the last years because of its superior sample throughput and high ionization efficiency.

Several sources of uncertainty, including memory effects, procedural blanks, mass bias, matrix effects, and reproducibility of the analysis, may compromise the accuracy of  $\delta^{11}\text{B}$  results obtained by MC-ICP-MS. The minimization of the impact of these uncertainty sources is particularly relevant to obtain meaningful results in samples containing nanogram boron amounts. Different strategies have been proposed to minimize memory effects arising from the volatility of boric acid: (1) the use of a direct injection high efficiency nebuliser (d-DIHEN), or its miniaturization ( $\mu$ -dDIHEN) [16–19]; (2) the addition of HF to the sample matrix [20,21] or NaF to the rinse solution [22] in order to generate the non-volatile boron tetrafluoride anion; (3) the introduction of ammonia gas in the spray chamber, so that the basic atmosphere inside the spray chamber converts boric acid into non-volatile borate ion [23,24].

Low procedural blanks are also mandatory, which requires several precautions during sample preparation. On the one hand, purified chemical reagents must be used, and it is highly recommended to install cartridges in the water purification systems specially designed to remove boron. On the other hand, samples must be prepared in clean room facilities, preferably with PTFE HEPA boron free filters rather than normal borosilicate HEPA filters.

During the analysis through MC-ICP-MS, boron fractionates in the spectrometer because of the mass bias intrinsically associated with this technique. This mass bias needs to be corrected analysing the NIST SRM 951a standard before and after each sample and using the standard-sample bracketing (SSB) approach [17,25]. However, prior to analysis, boron must be separated from the sample matrix to avoid unquantifiable matrix effects leading to a mass bias [26] non-correctable through the SSB approach. Whatever the purification method used, it is necessary to achieve complete boron recovery, which otherwise can lead to isotopic fractionation [27]. There are basically two alternatives for boron purification: the use of ion-exchange resins, such as the boron-specific Amberlite IRA-743 resin [14,24], and the so-called micro-distillation or microsublimation method [15,28]. The latter method is preferable for samples containing nanogram amounts of B, since procedural blanks can be reduced from over 100 pg [14,22,23,26] to approximately 10 pg [15, 19,20,28,29]. However, the boron amounts purified by micro-distillation are limited by the maximum volume of solution that

can be processed (30–70  $\mu\text{L}$ ) [19]. Note though that an alternative technique called macrosublimation has been proposed for samples containing lower boron concentrations, such as some natural waters, since it allows the processing of solution volumes one order of magnitude larger than micro-distillation [30].

Finally, the reproducibility of the analysis for a given boron amount depends on the sensitivity of each individual instrument and the combination of sample introduction and ion beam detection systems. For instance, the use of more efficient sample introduction systems, such as d-DIHEN and  $\mu$ -dDIHEN, can enhance the sensitivity, allowing the improvement of the measurement reproducibility for small boron amounts [16–19]. Furthermore, the use of  $10^{12}$  or  $10^{13}$   $\Omega$  amplifier resistors on the Faraday cups [21,24] as well as the detection of  $^{11}\text{B}$  and  $^{10}\text{B}$  signals with ion counters [15] has made possible to obtain measurement precisions better than 0.3 ‰ (2SD) at nanogram amounts using standard sample introduction systems.

In this study, we have assessed, for the first time, the performance of the Nu Instruments Plasma 3 MC-ICP-MS for  $\delta^{11}\text{B}$  determinations using different sample introduction systems and detector configurations. The primary goal is to present a detailed methodology for nanogram-scale boron isotope determination through a straightforward approach that can be easily adopted. Three sample introduction systems have been compared in terms of background intensity, sensitivity, efficiency and external reproducibility for B amounts ranging from ~0.7–36 ng. Two detector configurations were used based on the total boron signal intensity. The first configuration combines two Faraday cups fitted to  $10^{11}$   $\Omega$  and  $10^{12}$   $\Omega$  amplifier resistors for  $^{11}\text{B}$  and  $^{10}\text{B}$ , respectively. With the second configuration, we explored the potential of obtaining accurate  $\delta^{11}\text{B}$  results for B amounts below 4 ng by combining the detection of  $^{11}\text{B}$  on a Faraday cup (with a  $10^{12}$   $\Omega$  amplifier resistor) and  $^{10}\text{B}$  on an ion counter. Our approach has been validated through the analysis of solutions with varying boron concentrations. This includes boric acid in-house and standard reference materials, as well as four carbonate-matrix reference materials and two in-house carbonate-matrix standards purified by micro-distillation. Furthermore, we have studied the limits of the micro-distillation method in terms of the maximum carbonate mass that can be micro-distilled with complete boron recovery and lack of boron isotopic fractionation, which is critical for highly accurate  $\delta^{11}\text{B}$  determinations in low abundance carbonate samples.

## 2. Methods

### 2.1. Reagents, solutions and labware

All chemical and sample preparation steps were carried out in the Laboratori d'Isòtops Radiogènics i Ambientals (LIRA) at the University of Barcelona, which encompasses an ISO 7 clean laboratory with ISO 5 laminar flow hoods. Ultrapure water (UP water, 18.2 M $\Omega$  cm) was produced with a Genie G system (RephiLe Bioscience, Ltd.) with a boron removal cartridge. PrimarPlus - Trace analysis grade Nitric acid >68 % (Fisher Scientific) was double distilled in a DST-1000 Acid Purification System (Savillex) to ensure low boron blank levels. Ultrapure Hydrofluoric acid 48 % was purchased from Scharlab. Whenever solutions were exposed to the atmosphere, operations were carried out in the ISO 5 vented laminar flow hoods. Micro-distillation was performed over Analab hotplates placed inside Analab evaporation stations equipped with standard borosilicate HEPA filters.

The 5 mL conical-shape Savillex Teflon vials and lids used for micro-distillation were cleaned in a five-step protocol, with each of the first four steps followed by a triple rinse with UP water: (1) washed with neutral soap; (2) submerged in 50 % isopropyl alcohol for 1 h; (3) filled up until approximately half of their volume with aqua regia, and placed upside down with the closed lid overnight on a hotplate at 120 °C; (4) repetition of step 3 with 0.3 M  $\text{HNO}_3$  + 0.25 M HF; (5) Finally, vials and lids were manually shaken, the remaining water drops were removed with a pipette, and they were totally dried upside down on a hotplate

from the evaporation stations at 120 °C for 5 min, leaving a small gap between the vial and the lid, so that the vapor could escape with minimum atmosphere exposure.

Polypropylene (PP) vials and pipette tips were submerged in HNO<sub>3</sub> 10 % for 24 h. Additionally, PP vials were later filled up with 0.3 M HNO<sub>3</sub> + 0.25 M HF for 24 h. After each step, all of them were triple rinsed with UP water. Finally, they were manually shaken to remove water drops and dried in an ISO 5 vented laminar flow hood. Prior to using, pipette tips were also triple rinsed with the same clean reagent present in the acid matrix of the subsequently pipetted solution.

## 2.2. Boron recovery via micro-distillation

Boron was recovered from the carbonate matrix of the dissolved samples utilizing the micro-distillation technique. This approach is based on the volatility of boric acid, the predominant boron species in acid media. At low pH (<2), 100 % of boron is in the form of boric acid and can be distilled or sublimated at temperatures >65 °C [29,31]. The protocol used was adapted from methods described in the literature [15, 19,20,28,31]. Briefly, 40 µL of solution in a 0.3 M HNO<sub>3</sub> matrix was loaded on the centre of the lid of a clean 5 mL conical-shape Savillex Teflon vial with fin legs and tightly closed upside down. The vial was then wrapped with aluminium foil except for its conical tip to facilitate the condensation of the distilled boron in this colder part. Afterwards, it was placed upside down on a hotplate at 95 °C for a minimum of 15 h to perform the micro-distillation (see this choice of variables in the discussion below). Boron was collected in the conical top of the vial, whereas all non-volatile matrix components remained on the lid (Fig. 1). Thereafter, the vial was left to cool down (~45 min) and then was carefully turned over. The lid was subsequently replaced with a clean one, 140 µL of a 0.3 M HNO<sub>3</sub> + 0.3 M HF solution was added to the purified boron solution, and the final mixture was transferred to a clean 2 mL PP vial. A 10 µL aliquot of this solution was diluted to 100 µL with 0.3 M HNO<sub>3</sub> + 0.3 M HF for boron concentration determination prior to isotopic analysis.

## 2.3. Standard and reference materials

Boron isotopic composition is conventionally given in delta notation as parts per thousand deviations from the <sup>11</sup>B/<sup>10</sup>B value of the certified reference material (CRM) boric acid NIST SRM 951a [32], as follows:

$$\delta^{11}\text{B}(\text{‰}) = \left[ \frac{(^{11}\text{B}/^{10}\text{B})_{\text{sample}}}{(^{11}\text{B}/^{10}\text{B})_{\text{NIST SRM 951a}}} - 1 \right] \times 1000$$

NIST SRM 951a was purchased from the National Institute of Standards & Technology (NIST, USA). For the determination of the external reproducibility, an <sup>11</sup>B enriched in-house boric acid standard (11B-951) was prepared by adding a <sup>11</sup>B boric acid spike (kindly provided by Jugdeep Aggarwal) to a NIST SRM 951a solution. The δ<sup>11</sup>B of the 11B-951 standard was 15.2 ‰ to simulate a typical marine carbonate δ<sup>11</sup>B value [33].

A<sup>10</sup>B-enriched boron isotopic standard solution purchased from ISC Science was used as a spike for the determination, through Isotope Dilution (ID), of the boron yields obtained by micro-distillation.

Based on Raitzsch et al. [15], a carbonate simulated solution, CSS-1, was prepared from major elements standards (purchased from Inorganic Ventures) and NIST SRM 951 to verify that full boron recoveries were achieved via micro-distillation. It contained 2000 µg/mL of Ca, 800 ng/mL of Mg, Sr and Na, and 1250 ng/mL of B in 0.3 M HNO<sub>3</sub>, leading to 50 ng of B in the micro-distilled solution.

The micro-distillation technique and the analytical approaches implemented in this work were further validated by the processing of six carbonate-matrix standards: The Geological Survey of Japan reference materials (1) JCT-1 (*Tridacna gigas* giant clam) and (2) JCP-1 (*Porites* sp. coral) [34], the synthetic marine carbonate reference materials (3) NIST RM 8301 Foram and (4) NIST RM 8301 Coral [35], and two in-house carbonate-matrix standards (further details below), (5) CLD-1 (*Cladocora caespitosa* coral) and (6) GINF-1 (*Globoconella inflata* foraminifera).

Various JCT-1 (B/Ca ~191 µmol mol<sup>-1</sup>) and JCP-1 (B/Ca ~460 µmol mol<sup>-1</sup>) [34] aliquots were independently dissolved in HNO<sub>3</sub>, without prior chemical cleaning, and subsequently diluted to solutions containing 2 and 20 ng of B for JCT-1, and 3 and 20 ng of B for JCP-1, in a final acid matrix concentration of 0.3 M HNO<sub>3</sub>.

NIST RM 8301 Foram (B/Ca ~139 µmol mol<sup>-1</sup>) and NIST RM 8301 Coral (B/Ca ~528 µmol mol<sup>-1</sup>) are supplied dissolved in approximately 3.3 M HNO<sub>3</sub> to a final acid concentration of 1.8 M [35]. These materials were diluted with UP water to a final HNO<sub>3</sub> of 0.3 M. The micro-distilled 40 µL of these solutions contained approximately 15 and 60 ng of B, respectively.

The CLD-1 in-house standard (B/Ca ~660 µmol mol<sup>-1</sup>) was prepared through careful powdering and homogenization of *C. caespitosa* polyps from the Mediterranean Sea, previously oxidised using 30 % H<sub>2</sub>O<sub>2</sub>. Various CLD-1 batches were dissolved with HNO<sub>3</sub> independently, leading to a final acid concentration of 0.3 M; they were then split into aliquots that were purified via micro-distillation and analysed loading from 14 to 36 ng of B in the micro-distilled 40 µL sample).

To prepare the GINF-1 standard (B/Ca ~50 µmol mol<sup>-1</sup>), 31.5 mg of *G. inflata* foraminifera from ODP189 1171C-1H-03 sediment core were picked and gently crushed between two glass plates to crack open the chambers. Fragmented foraminifera were chemically cleaned following Pena et al. [36], including (1) clay removal, (2) oxidative cleaning with a 1 % H<sub>2</sub>O<sub>2</sub> solution buffered with 0.1 M NaOH, and (3) weak acid leaching in 0.001 M HNO<sub>3</sub>. Foraminifera were then dissolved to reach a concentration of 0.3 M HNO<sub>3</sub> and split into sixteen aliquots containing carbonate masses of 1, 1.5, 2, 2.5 and 3 mg. Each solution was micro-distilled to test the effectiveness of this technique using different carbonate masses. Given the small boron concentration in this sample, aliquots of 1 and 1.5 mg of carbonate were then mixed in pairs previous to analysis, so that the final boron concentration of the analysed solutions was similar to aliquots containing 2 and 3 mg, respectively. This was done to improve the precision of the results for aliquots with 1 and 1.5 mg, which contained less than 10 ng of boron. Finally, δ<sup>11</sup>B was measured in twelve final subsamples with boron masses ranging from 11

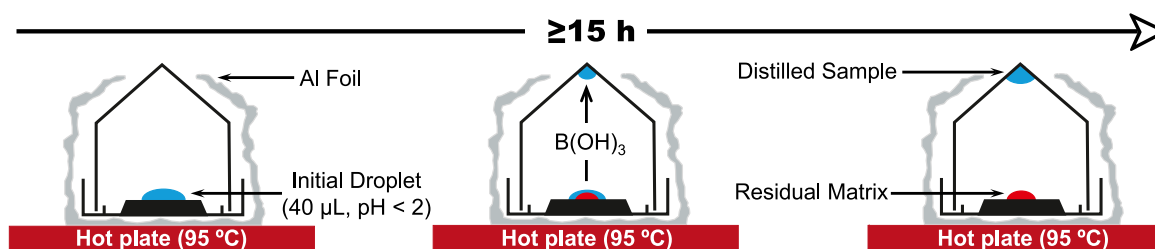


Fig. 1. Schematic illustration of the micro-distillation protocol used for B recovery from the carbonate matrix of the dissolved samples. Modified from Gaillardet et al. [31] and Buisson et al. [19].

to 16 ng.

Moreover, the boric acid reference material ERM-AE121 (BAM, Berlin, Germany) [37] was analysed as an additional quality control during different sessions. The measured aliquots contained between 14 and 32 ng of B.

#### 2.4. Boron isotope ratio measurements

Boron isotopic composition was analysed at the University of Barcelona PANTHALASSA facility using a Plasma 3 MC-ICP-MS (Nu Instruments). The main innovations incorporated into our instrument, compared to previous models, included an all-new ICP source that provides greater stability and ease of use, along with switchable resistors for Faraday cup preamplifiers, offering additional flexibility. This instrument was equipped with 18 detectors (16 Faraday cups and two Ion counters) as well as a switchable amplifier bin housing one  $10^{11} \Omega$  resistor for each amplifier and six  $10^{12} \Omega$  resistors at fixed positions. It was possible to quickly and automatically switch from  $10^{11}$  to  $10^{12} \Omega$  resistors for those amplifiers fitted to both types of resistors. The Cup configurations used in this work are shown in Table S1. In one of these configurations (FC11/FC12), two Faraday cups (H8 and L4) fitted to  $10^{11} \Omega$  and  $10^{12} \Omega$  amplifier resistors were used to detect the  $^{11}\text{B}$  and  $^{10}\text{B}$  ion beams, respectively. The second configuration (FC12/IC) was tested only for solutions leading to  $^{10}\text{B}$  signals lower than 14 mV (i.e.,  $\sim 800,000$  cps). Larger signals are not recommended to avoid the quick degradation of the ion counter. In this case, an ion counter (IC1) was used to detect the ion beam for  $^{10}\text{B}$  and a Faraday cup (H7) fitted to a  $10^{12} \Omega$  amplifier resistor for  $^{11}\text{B}$ . Since our system only had ion counters on one side of the detectors array, it was not possible to use ion counters for both isotopes, as proposed by Raitzsch et al. [15]. A preamplifier gain calibration was carried out before each measurement session. When the ion counter was used, a calibration between the responses of the Faraday cups and IC1 was also carried out daily. For this, a dynamic method was applied using a solution providing a signal for  $^{10}\text{B}$  of  $\sim 1.0$  Mcps. During the first cycle,  $^{11}\text{B}$  and  $^{10}\text{B}$  were collected on Faradays cups H8 and L5, respectively, while configuration FC12/IC was used for the second cycle. The detector baseline (background) was measured by ESA deflection for 180 s before both cycles and corrected. The FC/IC gain was obtained by dividing the  $^{11}\text{B}/^{10}\text{B}$  ratio measured in the second cycle from that obtained in the first cycle. Each time the ion counter voltage had to be increased due to aging, the dead time was measured, and a new value was set. The determination of the dead time was carried out according to Nelms et al. [38], specifically using Method 2. We analysed a solution containing natural uranium at various concentrations, with isotope  $^{238}\text{U}$  measured using a FC, and isotope  $^{235}\text{U}$  quantified using the IC, while limiting the signal for  $^{235}\text{U}$  in the IC to 1.0 Mcps. The procedure was replicated 8–10 times, and the average of the dead time values obtained were used. Typical uncertainties with this method were 1–2 ns (2SD).

Three different configurations of the sample introduction system have been compared in this study: (1) a Peltier-cooled ( $7^\circ\text{C}$ ) 50 mL inner-volume glass Twister spray chamber (Glass expansion) and a PFA-100 nebuliser (Elemental Scientific) with an uptake rate of  $170 \mu\text{L min}^{-1}$  (Glass-170 system); (2) a Scott type PFA spray chamber (Agilent) and a PFA-C50 nebuliser (Savilleux) with an uptake rate of  $50 \mu\text{L min}^{-1}$  (PFA-50 system); and (3) the same Scott PFA spray chamber with a PFA-20 MicroFlow Nebuliser (Elemental Scientific) with an uptake rate of  $30 \mu\text{L min}^{-1}$  (PFA-30 system). In the case of the PFA-30 system, a Perspex enclosure shielding the sample introduction system was used to reduce the impact of changes in the laboratory temperature on  $^{11}\text{B}/^{10}\text{B}$  reproducibility. A standard torch was used with the Glass-170 system, whereas a demountable torch with a 1.8 mm sapphire injector was used with the PFA-50 and PFA-30 systems. For all sample introduction system configurations, a standard nickel sampler cone (1.15 mm hole, 319–645) and a nickel WA7 skimmer cone (0.7 mm hole, 319–595) were used. A 2-mm spacer was installed on the skimmer cone mount, which provides an enhanced sensitivity for light elements. All solutions run with the Glass-

170 system were prepared in 0.3 M  $\text{HNO}_3$  matrix, whereas the matrix of solutions run with the PFA-50 and PFA-30 systems was 0.3 M  $\text{HNO}_3$  + 0.23 M HF.

Unless otherwise stated, samples and standards were acid and boron concentration matched to within  $\pm 10\%$ . Measurements were performed under low resolution mode (resolving power  $\sim 300$ ), since higher resolution was not required to resolve the  $^{10}\text{B}$  peak from  $\text{Ar}^{4+}$  and  $\text{Ne}^{2+}$  interferences. Each analysis consisted of a 120 s on-peak measurement of the background using an acid solution with the same matrix as the standards and samples, followed by the analysis of the sample/standard (60 cycles of 3 s). After each analysis, the sample introduction system was rinsed for 3 min with a wash solution with the same acid matrix as the samples and bracketing standards, before a new background measurement was carried out. For each set of analysed samples, the average signal of 3–5 procedural blanks run at the beginning of the measurement session was subtracted.

### 3. Results and discussion

#### 3.1. Procedural blanks

Boron concentration in reagents (UP water, 0.3 M  $\text{HNO}_3$  and 0.3 M HF) was  $\sim 0.1$  ppb ( $\sim 20$  pg of B in the final volume of each sample). This blank contribution was corrected as the same batch of acid was used for samples, bracketing standards and wash solution. The procedural blanks of the adopted micro-distillation protocol had a median of 12 pg of B (on average  $14 \pm 6$  pg, 1 SD,  $n = 27$ ), a negligible contribution that represents less than 0.5 % of a typical sample analysed with the FC12/IC configuration and less than 0.1 % of a typical sample analysed using the FC11/FC12 approach. These values are comparable to the lowest micro-distillation blanks reported in the literature [19,20,28,29], despite using normal borosilicate HEPA filters instead of boron free filters. This highlights that low blanks can be achieved when exhaustive vial cleaning protocols are performed and airborne exposure of samples is minimized, which is feasible using micro-distillation as the purification method.

#### 3.2. Mass bias stability, sensitivity, efficiency and signal-to-background ratio

The external reproducibility of  $\delta^{11}\text{B}$  measurements is influenced by different factors. For samples containing tens of nanograms of boron, the external reproducibility is usually limited by the mass bias stability of the instrument. Given the large relative mass difference among the two boron isotopes and the impossibility to use another pair of isotopes for the internal correction of mass bias, working under stable mass bias conditions is critical. Previous studies performed on the Neptune [25, 28] and Nu Plasma II [39] instruments reported a nebuliser pressure region where mass bias exhibited a plateau of stability. With the Plasma 3 instrument, however, we did not find this region of stability (Fig. S1), even scanning through nebuliser pressure ranges beyond those explored by Chen et al. [39] with the Nu Plasma II. Therefore, we always tuned the instrument to get maximum sensitivity. As stability tended to improve with functioning time, we monitored the ratios of the standard until optimal stability conditions were reached, and started measuring samples at this point. The lack of this mass bias stability region on Plasma 3 MC-ICMPS could be related to the modification of the ICP source compared to the Nu Plasma II. It must be noted that the Perspex enclosure shielding the sample introduction system significantly improved the stability of the temperature monitored in the torch box (maximum variations of  $0.5^\circ\text{C}$  within a measurement session) and the stability of the  $^{11}\text{B}/^{10}\text{B}$  measured for the NIST SRM 951a over time.

When boron amounts in the sample are reduced to a few nanograms, the ion beam intensity as well as the background level and stability can become the main factors limiting the external reproducibility [21]. In this case, using efficient sample introduction systems is critical. Fig. 2

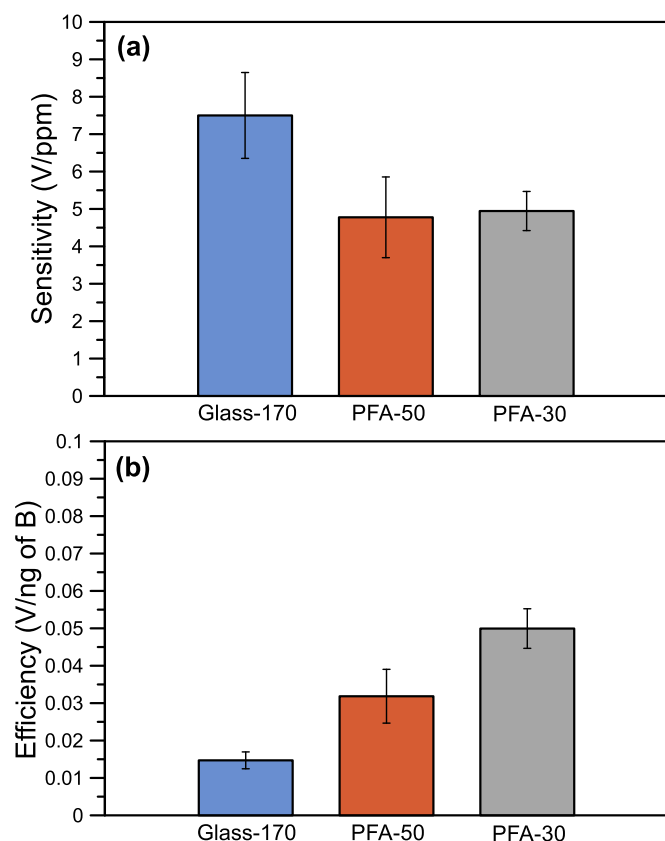


**Fig. 2.** Sensitivity (a), defined as  $^{10}\text{B} + ^{11}\text{B}$  signal in volts per ppb of B, and efficiency (b), defined as  $^{10}\text{B} + ^{11}\text{B}$  signal in volts per ng of B consumed during the measurement, for the three compared sample introduction systems (see main text). Error bars represent 2SD of external reproducibility. Data correspond to results obtained in  $n$  analytical sessions for each sample introduction system ( $n = 6$  for Glass-170;  $n = 12$  for PFA-50;  $n = 11$  for PFA-30).

compares the three sample introduction systems used in this study in terms of sensitivity (volts per ppb) and efficiency (volts per ng of B consumed during the analysis). It can be observed that, when considering the actual B consumed during the analysis, the PFA-30 system was 1.5 and 4 times more efficient than the PFA-50 and Glass-170 systems, respectively. This could result from the reported improvement in analyte transport efficiency shown by micronebulisers when decreasing the sample uptake rate [40]. In addition, it could result from other processes taking place in the sample introduction system, including the production of fine aerosols by micronebulisers and phenomena taking place inside the spray chamber, such as the enhancement in solvent evaporation and the decrease of droplet coalescence as the sample uptake rate is reduced [41].

In our study, the sensitivity obtained with the PFA-30 and PFA-50 systems led to a  $^{11}\text{B}$  signal of  $\sim 1.0$  Mcps on an ion counter for a 4 ppb B solution, which is similar to the signal reported by Raitzsch et al. [15] ( $\sim 1.3$  Mcps) with a Nu Plasma II using a  $50 \mu\text{L min}^{-1}$  nebuliser and a small-volume cyclonic quartz spray chamber. The background levels were, however, significantly improved in our study with the PFA-30 and PFA-50 systems compared to Raitzsch et al. [15] ( $\sim 10,000$  cps rather than 50,000 cps). This was probably due to the addition of HF to the samples and wash solutions. As it is shown in Figs. S2a and S2b, the addition of growing amounts of HF to the 0.3 M  $\text{HNO}_3$  solution significantly reduced the background, as previously reported [20,21], without any detrimental effect on sensitivity.

### 3.3. External reproducibility

For the determination of the external reproducibility of the measurement method, several replicates ( $n = 13\text{--}15$ ) of the in-house boric acid standard 11B-951 were analysed at different boron concentrations with the three sample introduction systems and the two detector configurations compared in this work. Based on Rae et al. [14], a weighted two-term exponential relationship was fitted to the results obtained with each set-up. In Fig. 3, external reproducibility (2SD) is plotted against the initial total mass of boron used for the analyses to compare the sample introduction systems in terms of needed sample amount. PFA-30 showed a superior performance, which is explained by its higher efficiency in terms of signal production per mass of B, as also shown in Fig. 2b. Therefore, this system was chosen in our usual procedure and was used for further analyses.

Following Rae et al. [14], we developed external reproducibility models from the correlation between the total boron signal intensity ( $[^{11}\text{B} + ^{10}\text{B}]$  in volts) and external reproducibility (2SD) of the boric acid measurements obtained using the PFA-30 system with FC11/FC12 and FC12/IC detector configurations. To achieve this, a weighted two-term exponential relationship was fitted to the results obtained with each configuration (Fig. 4). The resulting equations were used to assess sample  $\delta^{11}\text{B}$  reproducibility (2SD) from a single analysis, based on the  $[^{11}\text{B} + ^{10}\text{B}]$  signal of the sample. The calculations for each configuration are expressed as follows:

$$\text{FC11/FC12 : 2SD} = 0.45 \times \exp^{-0.79[^{11}\text{B} + ^{10}\text{B}]} + 36.46 \times \exp^{-42.69[^{11}\text{B} + ^{10}\text{B}]}$$

$$\text{FC12/IC : 2SD} = 0.57 \times \exp^{-6.64[^{11}\text{B} + ^{10}\text{B}]} + 3.06 \times \exp^{-88.79[^{11}\text{B} + ^{10}\text{B}]}$$

A statistically significant set of analyses of JCT-1 and RM 8301 Foram reference materials and the in-house standards CLD-1 and GINF-1 ( $n \geq 12$ ) were carried out at different boron concentrations to evaluate the impact of processing carbonate matrix samples in long-term reproducibility. The resulting total boron signal intensity and external reproducibility closely matched the external reproducibility models (Fig. 4b and c), suggesting that no additional significant uncertainty was introduced during chemical processing. Nevertheless, the procedural blank effect should not be neglected, particularly for samples containing nanogram boron amounts. For instance, in the analysis of JCT-1 replicates containing 3 ng of B, the procedural blanks ranged between 10 and 15 pg ( $n = 5$ ), and the reproducibility of  $\delta^{11}\text{B}$  results obtained for a single replicate by correcting the procedural blank contribution with each individual blank, rather than the average signal of the 5 procedural blanks was 0.06 ‰ (2SD). This value was negligible compared to the measurement reproducibility of 0.37 ‰ predicted by the model (Eq. 3). However, with higher blanks, like in a previous test performed with a diluted CSS-1 solution, the reproducibility of  $\delta^{11}\text{B}$  results obtained for a single replicate (also containing 3 ng of B) by correcting the blank contribution with each individual blank increased to 0.36 ‰, close to the measurement reproducibility. In such cases, both reproducibilities should be propagated quadratically to estimate the uncertainty of  $\delta^{11}\text{B}$  results. Note that the test with the CSS-1 solution was performed before implementing the step 5 of the Teflon vial cleaning protocol explained in section 2.1. In that case, the vials were finally dried open in the laminar flow hood, being exposed to the atmosphere for a couple of hours, and the procedural blanks increased to 20–30 pg. These results highlight the importance of minimizing the procedural blanks for samples containing nanogram boron amounts.

The best results at nanogram levels of B reported in the literature were achieved when highly efficient sample introduction systems were used, and the beams were detected with ion counters or  $10^{12}/10^{13} \Omega$  resistors on the amplifiers fitted to the Faraday Cups. Louvat et al. [16, 17] used a direct injection nebuliser (d-DIHEN): their best external reproducibilities were reported in Louvat et al. [17], ranging from 0.1 to 0.25 ‰, after analysing samples in triplicate and consuming 20 ng of B

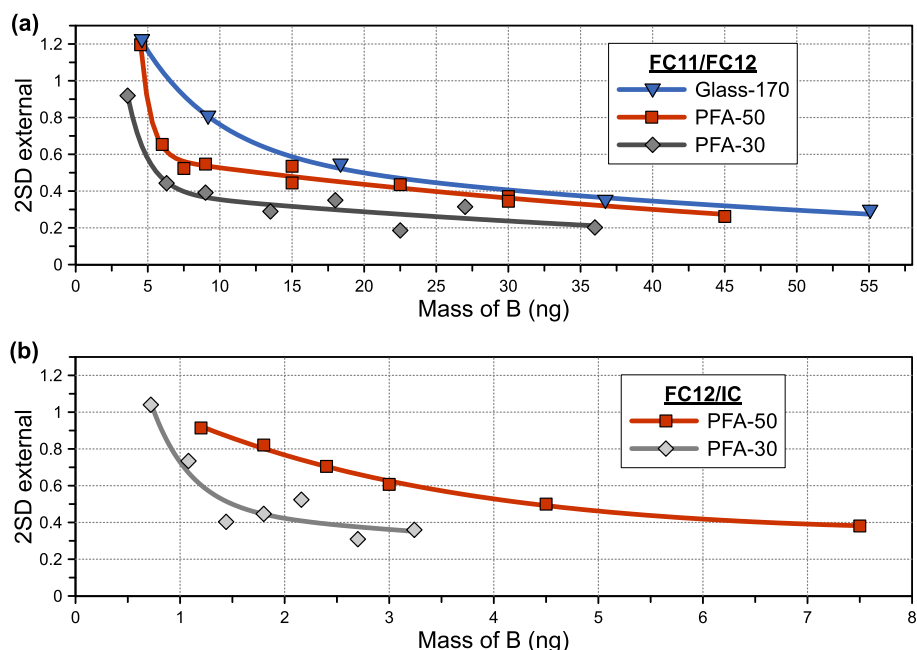


Fig. 3. External reproducibility (2SD,  $n = 13$ –15) of the in-house boric acid standard 11B-951 as a function of the initial boron mass. The analyses were conducted using Glass-170, PFA-50 and PFA-30 sample introduction systems, coupled with a) FC11/FC12 and (b) FC12/IC detector configurations.

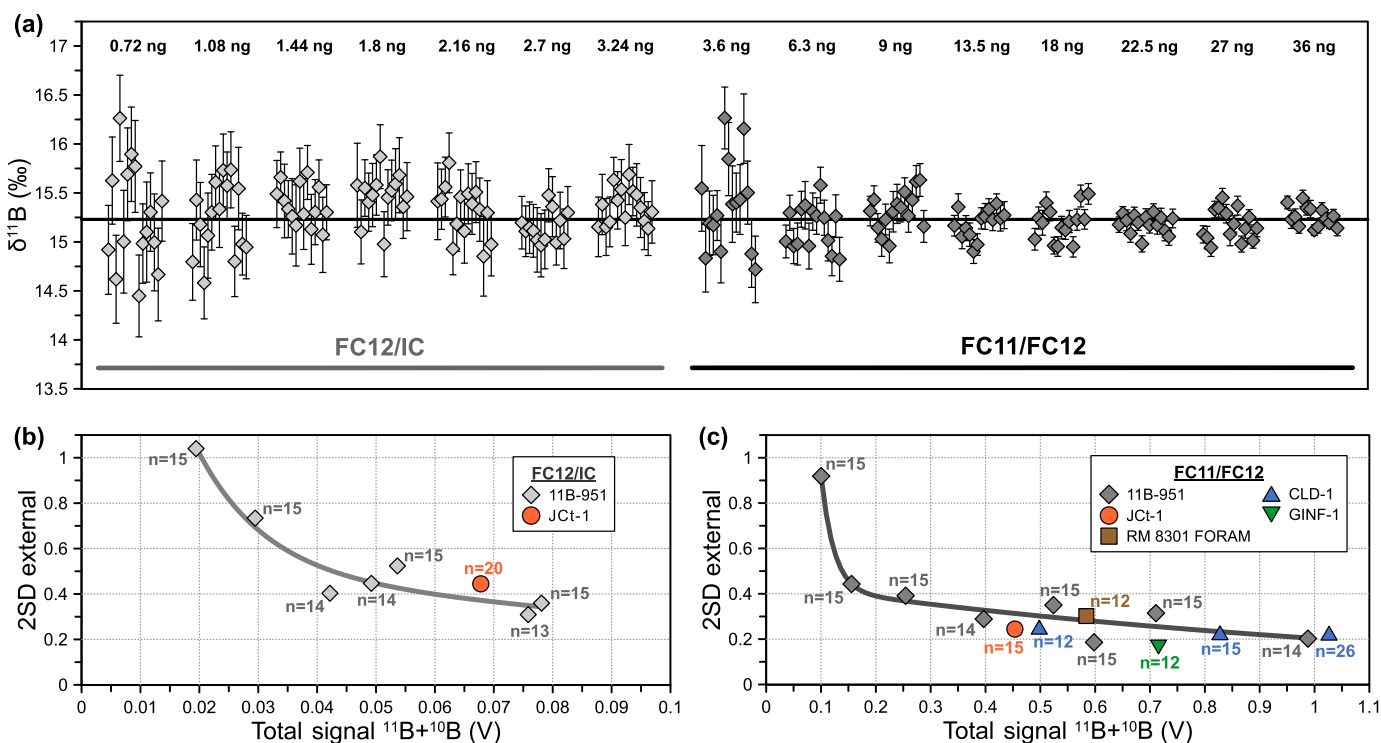


Fig. 4. (a)  $\delta^{11}\text{B}$  measurements of the in-house boric acid standard 11B-951. Analyses were carried out for differing boron masses utilizing the PFA-30 sample introduction system and the two detector configurations used in this work: FC12/IC and FC11/FC12 (see main text). For each measurement, the boron mass (ng) is shown above each group of analyses. Error bars represent two standard errors ( $2SE = 2SD/\sqrt{n}$ ) of internal measurement data. (b) External reproducibility model for the FC12/IC and (c) FC11/FC12 configurations were established from the relationship between the average total boron signal intensity (V) and the 2SD of the in-house boric acid standard in Fig. 4a, with different boron concentrations. A weighted two term exponential relationship was fitted to the boric acid data following Rae et al. [14]. Results from the analyses of Jct-1 and RM 8301 Foram reference materials and in-house standards CLD-1 and GINF-1 at a range of boron concentrations, processed through micro-distillation, are also plotted in Fig. 4b and c. The close match with the models suggests that no additional significant uncertainty was introduced during chemical processing.

per measurement. The analyte transport was 100 % with this nebuliser, since the aerosol was directly injected into the plasma, leading to a 2–3 times higher signal compared to a sample introduction system similar to

the PFA-50. In these set-ups, the higher linear velocity and larger size of droplets introduced into the plasma [16] may lead to a lower ionization efficiency. Louvat et al. [18] upgraded this system by developing the

$\mu$ -dDIHEN, a sample introduction setup with a d-DIHEN operating at flow rates as low as 5–7  $\mu\text{L min}^{-1}$ . A further advancement was made by Buisson et al. [19], where  $\mu$ -dDIHEN was combined with a sampler Jet cone, a skimmer X cone, and two  $10^{13} \Omega$  amplifiers, enhancing sensitivity and signal/noise ratio, and achieving  $\delta^{11}\text{B}$  reproducibilities of  $\pm 0.24 \text{‰}$  with 2.5 ng of boron and  $\pm 0.18 \text{‰}$  with boron masses between 2.5 and 5 ng. Raitzsch et al. [15] reported an external reproducibility of 0.3  $\text{‰}$  at best, with a minimum of 4 ng of boron using a sample introduction system similar to the PFA-50 and detecting both ion beams in ion counters. The alternative proposed by Jurikova et al. [42] also included an equivalent sample introduction system to the PFA-50, but with the use of  $10^{12} \Omega$  resistors on the Faraday cup amplifiers. A reproducibility of 0.2  $\text{‰}$  was reported for a minimum of 15 ng of B [42, 43]. Lloyd et al. [21] reported external reproducibilities of approximately 0.2  $\text{‰}$  with only 0.8–1.6 ng of boron. These authors combined the use of a sample introduction system similar to the PFA-30 and  $10^{13} \Omega$  resistors on the Faraday cup amplifiers for the detection of both ion beams. This set up was not available in our Plasma 3 MC-ICP-MS, so we explored the possibility of detecting the  $^{11}\text{B}$  beam on a Faraday cup fitted to a  $10^{12} \Omega$  amplifier resistor and the  $^{10}\text{B}$  beam on an ion counter using the FC12/IC configuration. As shown in Fig. 4, this option provided better measurement reproducibility than the FC11/FC12 approach for total boron signals below 0.35 V ( $\sim 12$  ng of B in the analysed solution).

### 3.4. Boron concentration matching

One of the factors potentially leading to inaccurate  $\delta^{11}\text{B}$  results is the mismatch between the boron concentration in the samples and the bracketing SRM 951a solution. Chen et al. [39] found that a 50 % mismatch in concentration led to biased results with a Nu Plasma II MC-ICP-MS. Louvat et al. [16] reported a bias of  $\delta^{11}\text{B} > 0.25 \text{‰}$  with a Neptune MC-ICP-MS when the mismatch was  $>20 \%$ , whereas other studies claimed that concentration matching was not needed with the Neptune [23,42]. We analysed a series of NIST SRM 951a solutions (taken as samples) at different boron concentrations using the same bracketing solution (standard) for all of them, varying the [sample]/[standard] ratio from 0.3 to 1.7. As shown in Fig. 5a, no bias was observed with the Plasma 3 MC-ICP-MS in this range of [sample]/[standard] ratios when the two ion beams were collected on Faraday cups. However, when the  $^{10}\text{B}$  ion beam was collected on an ion counter (FC12/IC configuration), a significant offset in the measured  $\delta^{11}\text{B}$  values was found for a concentration mismatch  $>30 \%$  (Fig. 5b). This was compatible with an overestimation of the ion counter dead time set value and, indeed, when we measured it again, we found it to be of 25 ns rather than 26 ns. With this new value, results improved significantly (Fig. 5c), but an offset was still evident on the low concentration range. Raitzsch et al. [15] used ion counters for the detection of both  $^{11}\text{B}$  and

$^{10}\text{B}$  ion beams and highlighted the need to match the sample and standard concentrations to within  $\pm 10 \%$  to ensure a similar background contribution on samples and standards. A background effect could also explain the offset shown in Fig. 5c at low concentrations but, still, a contribution of an incorrect dead time set value could not be ruled out. To illustrate the importance of accurately determining the dead time, we recalculated the  $\delta^{11}\text{B}$  values of Fig. 5c after correcting the  $^{10}\text{B}$  signals with different dead time values (Fig. S3). When applying a dead time value of 24 ns, the offset was lower than 0.2  $\text{‰}$ , whatever the [sample]/[standard] ratio. These results highlight the sensitivity of  $\delta^{11}\text{B}$  measurements to inaccurate dead time set values when ion counters are used as collectors: since the precision of dead time measurements was typically 1–2 ns (2SD), sample and standard concentrations were matched to within  $\pm 10 \%$  whenever the FC12/IC configuration was used for the analysis of samples. For the same reason, procedural blanks were always analysed using the cup configuration where  $^{10}\text{B}$  and  $^{11}\text{B}$  are detected on Faraday cups, in order to avoid biases associated to the non-linearity and dead time effects of the ion counters [44].

### 3.5. Acid matrix matching

Given the impact of the total boron signal on the measurement reproducibility (Fig. 4), minimizing the volume of samples to maximise the boron concentration was key to improve analytical uncertainty. Therefore, we decided to dissolve the samples in only 40  $\mu\text{L}$ , so that 100 % of the boron present in the sample could be micro-distilled. Afterwards, they were diluted with 0.3 M  $\text{HNO}_3$  + 0.3 M HF to 180  $\mu\text{L}$ , of which 10  $\mu\text{L}$  were used for boron concentration determination. The remaining 170  $\mu\text{L}$  were analysed for boron isotopes measurement, which was the minimum volume required for the PFA-30 system. This means that the samples were diluted only by factor 4.5 after the micro-distillation.

Several studies have demonstrated that differences in acid concentration between samples and bracketing standards could lead to significant biases in  $\delta^{11}\text{B}$  analyses [16,39,45,46], particularly when using HCl and  $\text{HNO}_3$ , but less evident for HF [45,46]. Fig. S4a shows the impact of a change in the  $\text{HNO}_3$  concentration in the sample with respect to the bracketing standard (0.3 M), while keeping the HF concentration constant. When the  $\text{HNO}_3$  concentration was 0.45 M, this bias was  $-0.39 \text{‰}$ , while it increased to over  $-1 \text{‰}$  for  $\text{HNO}_3$  concentrations higher than 0.6 M. These results agree with those previously obtained by Chen et al. [39, 45]. For this reason, ensuring that the  $\text{HNO}_3$  concentration in the micro-distilled solution was as close as possible to the bracketing standard was critical to avoid unsuitable acid matrix effects (Fig. S4a). This is why we established the following protocol: samples were dried and accurately weighed after the cleaning protocol. Then, they were dissolved in 40  $\mu\text{L}$  of  $\text{HNO}_3$ , with a concentration that varied depending on the sample mass, so that the expected final concentration was 0.3 M

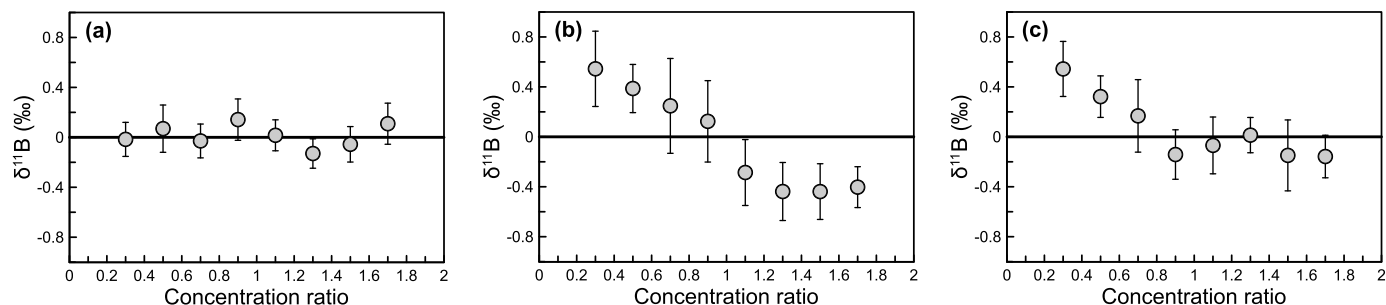


**Fig. 5.** Effect of B concentration mismatch on the measured  $\delta^{11}\text{B}$  for different ratios of B concentrations between the sample and the bracketing standard solution. A series of NIST SRM 951a solutions at different boron concentrations were analysed as samples and the same bracketing standard solution was used for all of them. (a)  $^{11}\text{B}$  and  $^{10}\text{B}$  signals measured on Faraday cups; (b)  $^{11}\text{B}$  signal measured on a Faraday cup and  $^{10}\text{B}$  signal measured on an ion counter with a dead time of 26 ns; (c)  $^{11}\text{B}$  signal measured on a Faraday cup and  $^{10}\text{B}$  signal measured on the same ion counter after determining a new dead time of 25 ns. The error bars correspond to 2SE ( $n = 7-8$ ).

(assuming a stoichiometry of 1:2 in the reaction between  $\text{CO}_3^{2-}$  and  $\text{H}^+$ ). For instance, samples containing 1, 2 or 3 mg of  $\text{CaCO}_3$  were dissolved with 40  $\mu\text{L}$  of 0.8, 1.3 or 1.8 M  $\text{HNO}_3$  solutions, respectively. Finally, the bracketing standards and wash solutions were prepared with the same batch of acid used for dissolving the samples.

To illustrate the importance of drying and weighing the samples after the cleaning protocol, we calculated the  $\text{HNO}_3$  concentration in the micro-distilled solution and the final solution analysed for three different scenarios of sample mass loss during the cleaning protocol (10, 20 and 30 %), assuming that the drying of the samples was not performed, and the nitric acid concentration used for the dissolution was that calculated from the initial sample mass and not from the true mass after cleaning. This simulation was performed for initial sample masses ranging between 1 and 5 mg (Figs. S4b and c). Afterwards, the expected  $\delta^{11}\text{B}$  bias caused by the  $\text{HNO}_3$  excess in the samples was estimated from the results of Fig. S4a. As it can be observed, this bias could exceed the measurement reproducibility depending on the initial sample mass and the mass loss during the cleaning protocol (Fig. S4d). Therefore, samples were systematically dried and weighed after cleaning to minimize this impact.

### 3.6. Boron purification by micro-distillation, choice of temperature and heating duration

The presence of elements such as calcium or magnesium in the samples can lead to inaccurate  $\delta^{11}\text{B}$  results [16,26]. For this reason, boron needs to be purified before analysing the samples through MC-ICP-MS. When samples contain only a few nanograms of boron, micro-distillation is a purification method providing exceptional performance, because procedural blanks with a few picograms of boron can be attained, as demonstrated by the present as well as previous studies [15,19,20,28,29]. However, full boron recovery is crucial, since incomplete recovery leads to a bias in  $\delta^{11}\text{B}$  due to the preferential condensation of the heavier isotope from the vapor phase, or its distillation from the original solution [20,47]. Different micro-distillation temperatures and heating durations have been suggested by other authors for full boron recovery [15,19,20,28,29,31]. Gaillardet et al. [31] proposed a temperature of 70 °C during 12–14 h. Wang et al. [28] fixed a standard micro-distillation duration of 12 h at 98 °C. Misra et al. [20] described a full boron recovery after 14 h at 75 °C, but ended up establishing the protocol at 95 °C for 18 h. Raitzsch et al. [15] set the protocol at 100 °C over 24 h. As Wang et al. [28] highlighted, complete recovery in Buisson et al. [19] was apparently achieved after 12 h, but at 95 °C; however, they extended the duration to 24 h at this temperature for practical reasons. Chanakya et al. [29] used a temperature of 99 °C for 20–24 h. Following Misra et al. [20] and Buisson et al. [19], we adopted a temperature of 95 °C with the aim of avoiding potential bubbling of the solution deposited on the vials lids. On the other hand, a heating duration of 15 h was chosen for time efficiency reasons, and was found appropriate after testing with the CSS-1 carbonate simulated solution. Micro-distilled aliquots contained 50 ng of boron, and the recoveries obtained, determined by isotope dilution, were  $99 \pm 5\%$  (2SD,  $n = 6$ ), verifying that full recovery was achieved under the test conditions. Therefore, a temperature of 95 °C and a heating duration of 15 h were established as our standard protocol for further analysis.

### 3.7. $\delta^{11}\text{B}$ measurements of reference materials

In order to check for  $\delta^{11}\text{B}$  biases due to matrix effects or isotopic fractionation during micro-distillation, and to evaluate the accuracy of the analytical procedure, repeat analyses of the carbonate-matrix reference materials Jct-1, JcP-1, RM 8301 Foram and RM 8301 Coral, and the boric acid ERM-AE121 were performed. The boron masses in the analysed solutions ranged from 2 to 58 ng, and the results are presented in Fig. 6. The measured  $\delta^{11}\text{B}$  values of Jct-1 with boron masses of 20 ng and 3 ng were  $16.33 \pm 0.24\%$  (2SD,  $n = 15$ ) and  $16.40 \pm 0.44\%$  (2SD,

$n = 18$ ), respectively (Fig. 6a and b). These results match the inter-laboratory value reported in Gutjahr et al. [34] for this material ( $16.39 \pm 0.60\%$ , un-oxidised). The average  $\delta^{11}\text{B}$  values of JcP-1 with boron masses of 20 ng and 2 ng were  $24.50 \pm 0.21\%$  (2SD,  $n = 6$ ) and  $24.33 \pm 0.47\%$  (2SD,  $n = 5$ ), respectively (Fig. 6c and d), both also in agreement with the consensus value published in Gutjahr et al. [34] ( $24.36 \pm 0.45\%$ , un-oxidised). Repeat analyses of the RM 8301 Foram (with 16 ng of B) resulted in a  $\delta^{11}\text{B}$  value of  $14.79 \pm 0.30\%$  (2SD,  $n = 12$ ; Fig. 6e), while the RM 8301 Coral average (with 58 ng of B) was  $24.43 \pm 0.25\%$  (2SD,  $n = 5$ ; Fig. 6f). It should be noted that our exact protocol could not be applied to both RM 8301 standards, as they are provided in solution (see Supplementary Note 1). Despite this, the results were consistent with the interlaboratory mean values reported in Stewart et al. [35] for these materials ( $14.49 \pm 0.39\%$  and  $24.17 \pm 0.35\%$ , respectively). The obtained  $\delta^{11}\text{B}$  value for ERM-AE121 was  $19.78 \pm 0.29\%$  (2SD,  $n = 16$ ), in accordance with the certified value ( $19.9 \pm 0.6\%$ ) [37]. Repeat analyses of these reference materials thus showed that no significant bias was observed, irrespective of the boron amount in the samples, validating our standard analytical procedure.

### 3.8. Maximum amounts amenable to micro-distillation and long-term reproducibility

An additional experiment (Fig. 7) was conducted to (1) test if our standard micro-distillation protocol enables full boron recovery regardless of the carbonate mass between 1 and 10 mg, and (2) evaluate the effect of varying heating time and carbonate mass on  $\delta^{11}\text{B}$ . It was performed on the basis that complete recovery of boron is achieved by micro-distillation of  $\sim 1$  mg of carbonate during 15 h at 95 °C. This was demonstrated from the accuracy of the replicate analysis of the Jct-1 with 20 ng of boron (purified from subsamples of 1.03 mg of carbonate), shown in section 3.7 (Fig. 6a).

We analysed subsamples of 1, 2, 3, 4, 5 and 10 mg of the CLD-1 standard, micro-distilled at 95 °C during 5, 15, 24 and 40 h. The aim was to establish the conditions providing non-significantly different results from the validated standard protocol: the  $\delta^{11}\text{B}$  value for aliquots of 1 mg of CLD-1, micro-distilled over 15 h, was  $25.67 \pm 0.23\%$ , 2SD,  $n = 42$  (Fig. 7a). As mentioned in section 3.6, incomplete B recovery leads to a bias in  $\delta^{11}\text{B}$ , resulting in a higher ratio. This was the case for CLD-1 subsamples of over 1 mg micro-distilled during only 5 h, for subsamples larger than 3 mg micro-distilled for 15 h, and for the 10 mg subsample micro-distilled during 24 h (Fig. 7a). On the contrary, solutions derived from the micro-distillation of up to 3 mg for a minimum of 15 h exhibited  $\delta^{11}\text{B}$  values within the 0.23 ‰ of the validated analytical reproducibility, indicating complete boron recovery. Hence, prolonged heating after achieving complete boron recovery does not seem to affect  $\delta^{11}\text{B}$ , indicating no significant sublimation of other elements from the carbonate matrix that could generate matrix effects during  $\delta^{11}\text{B}$  measurements, as found in Buisson et al. [19]. Micro-distillation of carbonate masses of 4 and 5 mg for at least 24 h and of 10 mg for 40 h seemed to allow for full B recoveries, although only one subsample per condition was analysed, so additionally tests would be required for further conclusions. A further test was conducted with subsamples of 1, 1.5, 2, 2.5 and 3 mg of the foraminifera GINF-1 standard micro-distilled at the same temperature for 15 h (Fig. 7b). Again, all  $\delta^{11}\text{B}$  values fell within the 2SD analytical reproducibility value of 1 mg aliquots ( $14.90 \pm 0.23\%$ , 2SD,  $n = 2$ ), displaying, altogether, a value of  $14.90 \pm 0.16\%$  (2SD,  $n = 12$ ). Furthermore, boron concentration was measured on the residual matrices by quadruple ICP-MS. In order to minimize matrix effects, they were diluted to 100 ppm of Ca. In addition, matrix matched standards were used both for the calibration line as well as bracketing standards. Internal standard correction (Rh) was also applied. This approach further minimises the potential matrix effect on these determinations. The boron concentrations found in the residual matrices were negligible, regardless of the micro-distilled carbonate mass. In conclusion, the proposed protocol, with a heating duration of at least 15

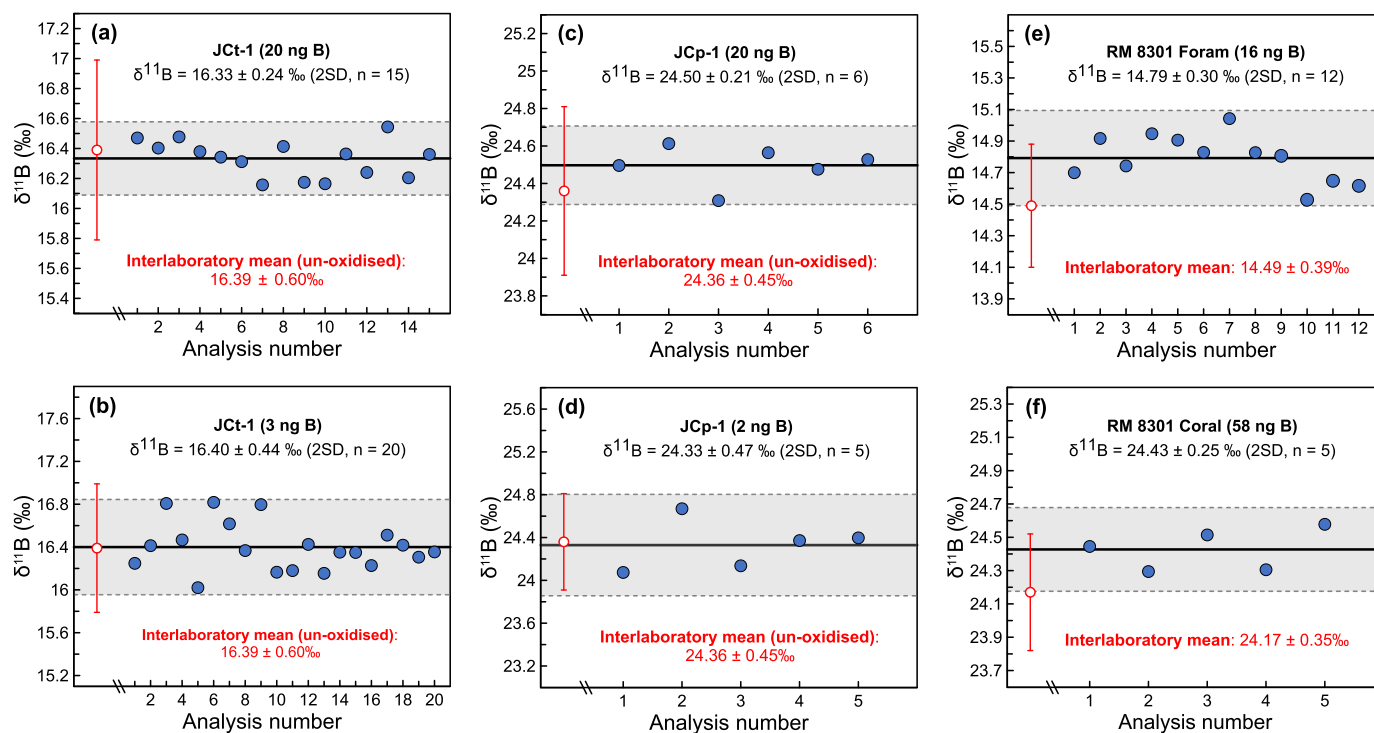


**Fig. 6.** Repeat analyses of the carbonate-matrix reference materials (a, b) JcT-1, (c, d) JcP-1, (e) RM 8301f and (f) RM 8301c. JcT-1 and JcP-1 were analysed at two different B concentrations; the boron masses (ng) of the aliquots are indicated in bold. The solid black lines represent the average of all measurements for each reference material (‰) and the grey bands cover the 2SD analytical reproducibility, also indicated in the upper part of each graph. The red open circles with red bars show the overall interlaboratory mean (‰) of un-oxidised JcT-1 and JcP-1 from Gutjahr et al. [34], and RM 8301 Foram and RM8301 Coral from Stewart et al. [35] (also indicated in red in the lower part of each graph).

h at 95 °C allows for complete boron recovery from up to 3 mg of carbonate mass.

Finally, the long-term reproducibility of  $\delta^{11}\text{B}$  measurements following our approach was assessed for the in-house carbonate standards CLD-1 as  $25.68 \pm 0.23$  ‰ (2SD,  $n = 53$ ; with 14–36 ng of B) and GINF-1 as  $14.90 \pm 0.16$  ‰ (2SD,  $n = 12$ ; with 11–16 ng of B).

#### 4. Conclusions

In this study, boron isotope analysis was set up using the Nu Plasma 3 MC-ICP-MS, for the first time. We focused on the analysis of marine biogenic carbonates, such as foraminifera and corals. Boron recovery was achieved through micro-distillation, with blanks displaying a median of 12 pg of B (on average  $14 \pm 6$  pg, 1 SD,  $n = 27$ ). Optimal conditions included a temperature of 95 °C and a minimum heating duration of 15 h, enabling the purification and recovery of boron from up to 3 mg of carbonate mass. The acid matrix of the sample solutions was 0.3 M  $\text{HNO}_3 + 0.23$  M HF. The addition of 0.23 M HF significantly reduced the background without compromising sensitivity.

Three sample introduction systems were tested, and the nebuliser system operating at  $30 \mu\text{L min}^{-1}$  exhibited superior performance in terms of signal intensity per mass of B compared to those at 50 and  $170 \mu\text{L min}^{-1}$ . Two detector configurations were used based on total boron signal intensity: (1) FC11/FC12, characterised by two Faraday cups fitted to  $10^{11} \Omega$  and  $10^{12} \Omega$  amplifier resistors to detect  $^{11}\text{B}$  and  $^{10}\text{B}$  ion beams, respectively, and (2) FC12/IC, with which we explored, for the first time, the viability of combining an ion counter and a Faraday cup fitted to a  $10^{12} \Omega$  amplifier to detect  $^{10}\text{B}$  and  $^{11}\text{B}$  ion beams, respectively. When the total boron signal was below 0.35 V ( $\sim 12$  ng of B in the solution), FC12/IC provided better measurement reproducibility.

The proposed analytical procedure requires strict control of procedural blanks and acid concentration matching between samples and the

bracketing standard. Validation involved processing and analysing reference materials, with results in line with interlaboratory exercises. Reference clam material JcT-1 yielded  $\delta^{11}\text{B}$  values of  $16.33 \pm 0.24$  ‰ (2SD,  $n = 15$ ; 20 ng of B) and  $16.40 \pm 0.44$  ‰ (2SD,  $n = 18$ ; 3 ng of B). Reference coral material JcP-1 showed  $\delta^{11}\text{B}$  values of  $24.50 \pm 0.21$  ‰ (2SD,  $n = 6$ ; 20 ng of B) and  $24.33 \pm 0.47$  ‰ (2SD,  $n = 5$ ; 2 ng of B). NIST RM 8301 Foram reference material had an average  $\delta^{11}\text{B}$  of  $14.79 \pm 0.30$  ‰ (2SD,  $n = 12$ ; 16 ng of B), and NIST RM 8301 Coral  $\delta^{11}\text{B}$  was  $24.43 \pm 0.25$  ‰ (2SD,  $n = 5$ ; 58 ng of B).

The long-term reproducibilities for our in-house carbonate standards CLD-1 and GINF-1 were  $25.68 \pm 0.23$  ‰ (2SD,  $n = 53$ ; 14–36 ng of B) and  $14.90 \pm 0.16$  ‰ (2SD,  $n = 12$ ; 11–16 ng of B), respectively.

Boron purification by micro-distillation and  $\delta^{11}\text{B}$  analysis using Nu Plasma 3 MC-ICP-MS proves valuable for paleo-pH reconstructions when only relatively low amounts of carbonate are available. We present a detailed methodology that can be easily adopted and is also applicable to other geochemical research areas.

#### Author contributions

**César Nicolás Rodríguez-Díaz:** Conceptualization, Methodology, Investigation, Writing - Original draft. **Eduardo Paredes:** Conceptualization, Methodology, Investigation, Writing - Original draft. **Leopoldo Peña:** Conceptualization, Methodology, Resources, Writing - Review & Editing, Funding acquisition. **Isabel Cacho:** Writing - Review & Editing, Resources, Funding acquisition. **Carles Pelejero:** Conceptualization, Methodology, Resources, Writing - Review & Editing, Supervision, Funding acquisition. **Eva Calvo:** Conceptualization, Methodology, Resources, Writing - Review & Editing, Supervision, Funding acquisition.

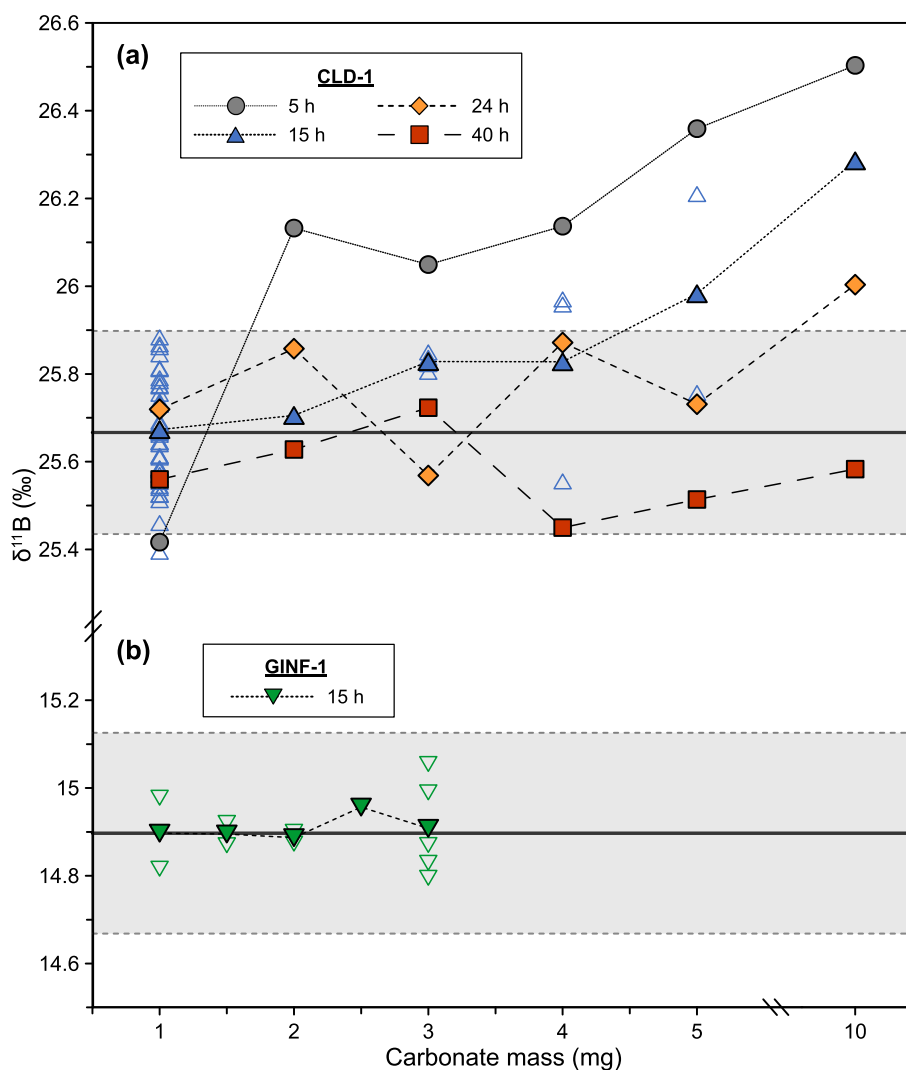


**Fig. 7.**  $\delta^{11}\text{B}$  measurements of our in-house coral and foraminiferal standards (a) CLD-1 and (b) GINF-1, as a function of the dissolved carbonate mass and the micro-distillation duration. The grey bands represent 2SD analytical reproducibility for aliquots of 1 mg carbonate micro-distilled over 15 h for both materials (CLD-1:  $25.67 \pm 0.23$  ‰, 2SD,  $n = 42$ ; GINF-1:  $14.90 \pm 0.23$  ‰, 2SD,  $n = 2$ ). Single  $\delta^{11}\text{B}$  measurements are displayed by unfilled symbols, while average  $\delta^{11}\text{B}$  values are shown as filled symbols (note that, when  $n = 1$ , the symbol also appears filled). The 2SD external reproducibility of the measurements varies between  $\pm 0.2$  and  $0.29$  ‰.

#### Declaration of competing interest

The authors declare that they have no known competing financial interests or personal relationships that could have appeared to influence the work reported in this paper.

#### Data availability

Data will be made available on request.

#### Acknowledgements

Financial support is acknowledged to the Spanish Ministry of Science and Innovation through research projects HICCUP (RTI2018-095083-B-I00), TRANSMOW (PID2019-105523RB-I00) and ESCACS (PID2021-122451OB-I00), and to European Research Council (Consolidator Grants) through research project TIMED (683237). C.N.R.-D. acknowledges an FPI PhD contract funded by the Spanish AEI. I.C. acknowledges an ICREA-Academia award. This work acknowledges the “Severo Ochoa Centre of Excellence” accreditation (CEX2019-000928-S) funded by AEI 10.13039/501100011033. This is a contribution from the Marine

Biogeochemistry and Global Change research group (Grant 2021SGR00430) and the Geociències Marines research group (Grant 2021SGR01195) from Generalitat de Catalunya.

#### Appendix A. Supplementary data

Supplementary data to this article can be found online at <https://doi.org/10.1016/j.talanta.2023.125473>.

#### References

- [1] K.J.R. Rosman, P.D.P. Taylor, Isotopic compositions of the elements 1997 (technical report), *Pure Appl. Chem.* 70 (1998) 217–235, <https://doi.org/10.1351/pac199870010217>.
- [2] L.B. Williams, R.L. Hervig, Boron isotope composition of coals: a potential tracer of organic contaminated fluids, *Appl. Geochem.* 19 (2004) 1625–1636, <https://doi.org/10.1016/j.apgeochem.2004.02.007>.
- [3] J.F. Hogan, J.D. Blum, Boron and lithium isotopes as groundwater tracers: a study at the fresh kills landfill, staten island, New York, USA, *Appl. Geochem.* 18 (2003) 615–627, [https://doi.org/10.1016/S0883-2927\(02\)00153-1](https://doi.org/10.1016/S0883-2927(02)00153-1).
- [4] J. Gaillardet, D. Lemarchand, Boron in the weathering environment, in: *Advances in Isotope Geochemistry*, Springer, 2018, pp. 163–188, [https://doi.org/10.1007/978-3-319-64666-4\\_7](https://doi.org/10.1007/978-3-319-64666-4_7).

- [5] J.C.M. De Hoog, I.P. Savov, Boron isotopes as a tracer of subduction zone processes, in: *Advances in Isotope Geochemistry*, Springer, 2018, pp. 217–247, [https://doi.org/10.1007/978-3-319-64666-4\\_9](https://doi.org/10.1007/978-3-319-64666-4_9).
- [6] H.R. Marschall, Boron isotopes in the ocean floor realm and the mantle, in: *Advances in Isotope Geochemistry*, Springer, 2018, pp. 189–215, [https://doi.org/10.1007/978-3-319-64666-4\\_8](https://doi.org/10.1007/978-3-319-64666-4_8).
- [7] R.B. Trumbull, J.F. Slack, Boron isotopes in the continental crust: granites, pegmatites, felsic volcanic rocks, and related ore deposits, in: *Advances in Isotope Geochemistry*, Springer, 2018, pp. 249–272, [https://doi.org/10.1007/978-3-319-64666-4\\_10](https://doi.org/10.1007/978-3-319-64666-4_10).
- [8] G.L. Foster, J.W.B. Rae, Reconstructing Ocean pH with boron isotopes in foraminifera, *Annu. Rev. Earth Planet Sci.* 44 (2016) 207–237, <https://doi.org/10.1146/annurev-earth-060115-012226>.
- [9] J.W.B. Rae, Boron isotopes in foraminifera: systematics, biomineralisation, and CO<sub>2</sub> reconstruction, in: *Advances in Isotope Geochemistry*, Springer, 2018, pp. 107–143, [https://doi.org/10.1007/978-3-319-64666-4\\_5](https://doi.org/10.1007/978-3-319-64666-4_5).
- [10] B. Hönisch, S.M. Eggins, L.L. Haynes, K.A. Allen, K.D. Holland, K. Lorbacher, Boron Proxies in Paleoclimatology and Paleoclimatology, John Wiley & Sons, Ltd, Chichester, UK, 2019, <https://doi.org/10.1002/9781119010678>.
- [11] G.L. Foster, Y. Ni, B. Haley, T. Elliott, Accurate and precise isotopic measurement of sub-nanogram sized samples of foraminiferal hosted boron by total evaporation NTIMS, *Chem. Geol.* 230 (2006) 161–174, <https://doi.org/10.1016/j.chemgeo.2005.12.006>.
- [12] G. Wei, M.T. McCulloch, G. Mortimer, W. Deng, L. Xie, Evidence for ocean acidification in the great barrier reef of Australia, *Geochim. Cosmochim. Acta* 73 (2009) 2332–2346, <https://doi.org/10.1016/j.gca.2009.02.009>.
- [13] J. Xiao, Y. Xiao, Z. Jin, C. Liu, M. He, Boron isotopic compositions in growing corals from the South China Sea, *J. Asian Earth Sci.* 62 (2013) 561–567, <https://doi.org/10.1016/j.jseas.2012.11.005>.
- [14] J.W.B. Rae, G.L. Foster, D.N. Schmidt, T. Elliott, Boron isotopes and B/Ca in benthic foraminifera: proxies for the deep ocean carbonate system, *Earth Planet Sci. Lett.* 302 (2011) 403–413, <https://doi.org/10.1016/j.epsl.2010.12.034>.
- [15] M. Raitzsch, J. Bijma, A. Benthien, K.-U. Richter, G. Steinhoefel, M. Kučera, Boron isotope-based seasonal paleo-pH reconstruction for the Southeast Atlantic – a multispecies approach using habitat preference of planktonic foraminifera, *Earth Planet Sci. Lett.* 487 (2018) 138–150, <https://doi.org/10.1016/j.epsl.2018.02.002>.
- [16] P. Louvat, J. Bouchez, G. Paris, MC-ICP-MS isotope measurements with direct injection nebulisation (d-DIHEN): optimisation and application to boron in seawater and carbonate samples, *Geostand. Geoanal. Res.* 35 (2011) 75–88, <https://doi.org/10.1111/j.1751-908X.2010.00057.x>.
- [17] P. Louvat, J. Moureau, G. Paris, J. Bouchez, J. Noireaux, J. Gaillardet, A fully automated direct injection nebulizer (d-DIHEN) for MC-ICP-MS isotope analysis: application to boron isotope ratio measurements, *J. Anal. At. Spectrom.* 29 (2014) 1698–1707, <https://doi.org/10.1039/C4JA00098F>.
- [18] P. Louvat, M. Tharaud, M. Buisson, C. Rollion-Bard, M.F. Benedetti,  $\mu$ -dDIHEN: a new micro-flow liquid sample introduction system for direct injection nebulization in ICP-MS, *J. Anal. At. Spectrom.* 34 (2019) 1553–1563, <https://doi.org/10.1039/C9JA00146H>.
- [19] M. Buisson, P. Louvat, C. Thaler, C. Rollion-Bard, High precision MC-ICP-MS measurements of <sup>11</sup>B/<sup>10</sup>B ratios from ng amounts of boron in carbonate samples using microsublimation and direct injection ( $\mu$ -dDIHEN), *J. Anal. At. Spectrom.* 36 (2021) 2116–2131, <https://doi.org/10.1039/D1JA00109D>.
- [20] S. Misra, R. Owen, J. Kerr, M. Greaves, H. Elderfield, Determination of <sup>11</sup>B by HR-ICP-MS from mass limited samples: application to natural carbonates and water samples, *Geochim. Cosmochim. Acta* 140 (2014) 531–552, <https://doi.org/10.1016/j.gca.2014.05.047>.
- [21] N.S. Lloyd, A.Yu Sadekov, S. Misra, Application of 10<sup>13</sup> ohm Faraday cup current amplifiers for boron isotopic analyses by solution mode and laser ablation multicollector inductively coupled plasma mass spectrometry, *Rapid Commun. Mass Spectrom.* 32 (2018) 9–18, <https://doi.org/10.1002/rcm.8009>.
- [22] M.-Y. He, L. Deng, H. Lu, Z.-D. Jin, Elimination of the boron memory effect for rapid and accurate boron isotope analysis by MC-ICP-MS using NaF, *J. Anal. At. Spectrom.* 34 (2019) 1026–1032, <https://doi.org/10.1039/C9JA00007K>.
- [23] G.L. Foster, B. Hönisch, G. Paris, G.S. Dwyer, J.W.B. Rae, T. Elliott, J. Gaillardet, N. G. Hemming, P. Louvat, A. Vengosh, Interlaboratory comparison of boron isotope analyses of boric acid, seawater and marine CaCO<sub>3</sub> by MC-ICPMS and NTIMS, *Chem. Geol.* 358 (2013) 1–14, <https://doi.org/10.1016/j.chemgeo.2013.08.027>.
- [24] J.R. Farmer, B. Hönisch, J. Uchikawa, Single laboratory comparison of MC-ICP-MS and N-TIMS boron isotope analyses in marine carbonates, *Chem. Geol.* 447 (2016) 173–182, <https://doi.org/10.1016/j.chemgeo.2016.11.008>.
- [25] G.L. Foster, Seawater pH, pCO<sub>2</sub> and [CO<sub>3</sub><sup>2-</sup>] variations in the Caribbean Sea over the last 130 kyr: a boron isotope and B/Ca study of planktic foraminifera, *Earth Planet Sci. Lett.* 271 (2008) 254–266, <https://doi.org/10.1016/j.epsl.2008.04.015>.
- [26] C. Guerrot, R. Millot, M. Robert, P. Nègre, Accurate and high-precision determination of boron isotopic ratios at low concentration by MC-ICP-MS (Neptune), *Geostand. Geoanal. Res.* 35 (2011) 275–284, <https://doi.org/10.1111/j.1751-908X.2010.00073.x>.
- [27] D. Lemarchand, J. Gaillardet, C. Göpel, G. Manhès, An optimized procedure for boron separation and mass spectrometry analysis for river samples, *Chem. Geol.* 182 (2002) 323–334, [https://doi.org/10.1016/S0009-2541\(01\)00329-1](https://doi.org/10.1016/S0009-2541(01)00329-1).
- [28] B.-S. Wang, C.-F. You, K.-F. Huang, S.-F. Wu, S.K. Aggarwal, C.-H. Chung, P.-Y. Lin, Direct separation of boron from Na- and Ca-rich matrices by sublimation for stable isotope measurement by MC-ICP-MS, *Talanta* 82 (2010) 1378–1384, <https://doi.org/10.1016/j.talanta.2010.07.010>.
- [29] I.V.S. Chanakya, S. Misra, Accurate and precise determination of the boron isotope ratio by QQQ-ICP-MS: application to natural waters and carbonates, *J. Anal. At. Spectrom.* 37 (2022) 1327–1339, <https://doi.org/10.1039/D2JA00051B>.
- [30] T.-H. Wang, C.-F. You, C.-H. Chung, H.-C. Liu, Y.-P. Lin, Macro-sublimation: purification of boron in low-concentration geological samples for isotopic determination by MC-ICPMS, *Microchem. J.* 152 (2020), 104424, <https://doi.org/10.1016/j.microc.2019.104424>.
- [31] J. Gaillardet, D. Lemarchand, C. Göpel, G. Manhès, Evaporation and sublimation of boric acid: application for boron purification from organic rich solutions, *Geostand. Geoanal. Res.* 25 (2001) 67–75, <https://doi.org/10.1111/j.1751-908X.2001.tb00788.x>.
- [32] W.A. Brand, T.B. Coplen, J. Vogl, M. Rosner, T. Prohaska, Assessment of international reference materials for isotope-ratio analysis (IUPAC technical report), *Pure Appl. Chem.* 86 (2014) 425–467, <https://doi.org/10.1515/PAC-2013-1023/MACHNEREADABLECITATION/RIS>.
- [33] S.K. Aggarwal, C.-F. You, A review on the determination of isotope ratios of boron with mass spectrometry, *Mass Spectrom. Rev.* 36 (2017) 499–519, <https://doi.org/10.1002/mas.21490>.
- [34] M. Gutjahr, L. Bordier, E. Douville, J. Farmer, G.L. Foster, E.C. Hathorne, B. Hönisch, D. Lemarchand, P. Louvat, M. McCulloch, J. Noireaux, N. Pallavicini, J. W.B. Rae, I. Rodushkin, P. Roux, J.A. Stewart, F. Thil, C. You, Sub-permil interlaboratory consistency for solution-based boron isotope analyses on marine carbonates, *Geostand. Geoanal. Res.* 45 (2021) 59–75, <https://doi.org/10.1111/ggr.12364>.
- [35] J.A. Stewart, S.J. Christopher, J.R. Kucklick, L. Bordier, T.B. Chalk, A. Dapoigny, E. Douville, G.L. Foster, W.R. Gray, R. Greenop, M. Gutjahr, F. Hemming, M. J. Henehan, P. Holdship, Y. Hsieh, A. Kolevica, Y. Lin, E.M. Mawbey, J.W.B. Rae, L. F. Robinson, R. Shuttleworth, C. You, S. Zhang, R.D. Day, NIST RM 8301 boron isotopes in marine carbonate (simulated coral and foraminifera solutions): inter-laboratory  $\delta^{11}\text{B}$  and Trace element ratio value assignment, *Geostand. Geoanal. Res.* 45 (2021) 77–96, <https://doi.org/10.1111/ggr.12363>.
- [36] L.D. Pena, E. Calvo, I. Cacho, S. Eggins, C. Pelejero, Identification and removal of Mn-Mg-rich contaminant phases on foraminiferal tests: implications for Mg/Ca past temperature reconstructions, *G-cubed* 6 (2005), <https://doi.org/10.1029/2005GC000930>.
- [37] J. Vogl, M. Rosner, Production and certification of a unique set of isotope and delta reference materials for boron isotope determination in geochemical, environmental and industrial materials, *Geostand. Geoanal. Res.* 36 (2012) 161–175, <https://doi.org/10.1111/j.1751-908X.2011.00136.x>.
- [38] S.M. Nelms, C.R. Quétel, T. Prohaska, J. Vogl, P.D.P. Taylor, Evaluation of detector dead time calculation models for ICP-MS, *J. Anal. At. Spectrom.* 16 (2001) 333–338, <https://doi.org/10.1039/B007913H>.
- [39] X. Chen, F. Teng, D.C. Catling, Fast and precise boron isotopic analysis of carbonates and seawater using Nu Plasma II multi-collector inductively coupled plasma mass spectrometry and a simple sample introduction system, *Rapid Commun. Mass Spectrom.* 33 (2019) 1169–1178, <https://doi.org/10.1002/rcm.8456>.
- [40] J.-L. Todolí, V. Hernandis, A. Canals, J.-M. Mermet, Comparison of characteristics and limits of detection of pneumatic micronebulizers and a conventional nebulizer operating at low uptake rates in ICP-AES, *J. Anal. At. Spectrom.* 14 (1999) 1289–1295, <https://doi.org/10.1039/A900598F>.
- [41] J.L. Todolí, J.M. Mermet, Sample introduction systems for the analysis of liquid microsamples by ICP-AES and ICP-MS, *Spectrochim. Acta Part B At. Spectrosc.* 61 (2006) 239–283, <https://doi.org/10.1016/j.sab.2005.12.010>.
- [42] H. Jurikova, V. Liebetrau, M. Gutjahr, C. Rollion-Bard, M.Y. Hu, S. Krause, D. Henkel, C. Hiebenthal, M. Schmidt, J. Laudien, A. Eisenhauer, Boron isotope systematics of cultured brachiopods: response to acidification, vital effects and implications for palaeo-pH reconstruction, *Geochim. Cosmochim. Acta* 248 (2019) 370–386, <https://doi.org/10.1016/j.gca.2019.01.015>.
- [43] T. Müller, H. Jurikova, M. Gutjahr, A. Tomašových, J. Schlögl, V. Liebetrau, L. v. Duarte, R. Milovský, G. Suan, E. Mattioli, B. Pittet, A. Eisenhauer, Ocean acidification during the early Toarcian extinction event: evidence from boron isotopes in brachiopods, *Geology* 48 (2020) 1184–1188, <https://doi.org/10.1130/G47781.1>.
- [44] S. Richter, S. Konegger-Kappel, S.F. Boulyga, G. Stadelmann, A. Koepf, H. Siegmund, Linearity testing and dead-time determination for MC-ICP-MS ion counters using the IRMM-072 series of uranium isotope reference materials, *J. Anal. At. Spectrom.* 31 (2016) 1647–1657, <https://doi.org/10.1039/C6JA00203J>.
- [45] X. Chen, L. Zhang, G. Wei, J. Ma, Matrix effects and mass bias caused by inorganic acids on boron isotope determination by multi-collector ICP-MS, *J. Anal. At. Spectrom.* 31 (2016) 2410–2417, <https://doi.org/10.1039/C6JA00328A>.
- [46] M.T. McCulloch, M. Holcomb, K. Rankenburg, J.A. Trotter, Rapid, high-precision measurements of boron isotopic compositions in marine carbonates, *Rapid Commun. Mass Spectrom.* 28 (2014) 2704–2712, <https://doi.org/10.1002/rcm.7065>.
- [47] B. Chetelat, J. Gaillardet, R. Freydisier, P. Nègre, Boron isotopes in precipitation: experimental constraints and field evidence from French Guiana, *Earth Planet Sci. Lett.* 235 (2005) 16–30, <https://doi.org/10.1016/j.epsl.2005.02.014>.